A compact kinetic reaction mechanism for the oxidation of NH_3/H_2 mixtures

Ali Alnasif [a,b], Joanna Jójka J[c], Máté Papp[d], András G. Szanthoffer[d,e], Marina Kovaleva[a], Tamás Turányi[d], Syed Mashruk[a], Agustin Valera-Medina[a,*], Tibor Nagy[f,*]

[a] *College of Physical Sciences and Engineering, Cardiff University, Cardiff, CF24 3AA, United Kingdom*
[b] *Engineering Technical College of Al-Najaf, Al-Furat Al-Awsat Technical University, Najaf, 31001, Iraq*
[c] *Institute of Thermal Engineering, Poznan University of Technology, 60-965 Poznan, Poland*
[d] *Institute of Chemistry, ELTE Eötvös Loránd University, Budapest, 1117, Hungary*
[e] *Hevesy György PhD School of Chemistry, ELTE Eötvös Loránd University, Budapest, 1117, Hungary*
[f] *Institute of Materials and Environmental Chemistry, HUN-REN Research Centre for Natural Sciences, Budapest, 1117, Hungary*

Abstract

Ammonia (NH_3) has been considered a potential fuel for energy production to achieve zero carbon emissions. However, several challenges must be addressed to ensure its widespread use and safety. The current work focuses on developing a kinetic reaction mechanism that not only accurately predicts laminar flame speeds and the emissions from NH_3 and NH_3/H_2 flames across various conditions but also ensures seamless applicability in Computational Fluid Dynamics (CFD) simulations, particularly in scenarios involving turbulent flows, such as swirl burners or complex engine chamber conditions. Using code Optima++, the rate parameters of the San Diego NH_3 mechanism (only 21 species and 64 reactions) were optimised against a large collection of laminar burning velocity data, and concentration data measured in jet-stirred reactors and burner-stabilised stagnation flame experiments to develop a compact, yet robust model for CFD simulations. Due to its small size, the mechanism lacks important chemical pathways, so the requirement for physically realistic rate coefficients had to be sacrificed in order to achieve the best possible predictivity for practical applications. The mechanism has been tested for 70/30 vol% NH_3/H_2 mixtures in CFD simulations of a general swirl burner against experimentally measured concentrations. Its predictions demonstrated good qualitative and often quantitative agreement with the experimental data for NO, N_2O, and NO_2 emissions, and NH_3 slip in the whole equivalence ratio range, while allowing accelerated simulations compared to other leading mechanisms.

Keywords: Parameter optimisation, Laminar flame speed, Burner-stabilised stagnation flame, Jet-stirred reactor, Computational Fluid Dynamics

---

* ValeraMedinaA1@cardiff.ac.uk
nagy.tibor@ttk.hu

1. Introduction

Rising concerns over oil depletion and CO_2 emissions highlight the need for alternative fuels. Hydrogen (H_2) is promising but has safety risks [1], whereas ammonia (NH_3) is gaining attention as a carbon-free fuel with easier storage and transport than H_2, thanks to existing infrastructure and lower reactivity, and easy liquefaction [2–4]. However, NH_3 combustion faces challenges, including hazardous NO_x emissions under fuel-lean conditions [5,6], low burning velocity, and high ignition temperature. Blending with H_2 improves efficiency, but in fuel-rich mixtures unburned NH_3 slip remains a concern due to its toxicity and environmental impact [7].

Developing efficient, low-emission combustion systems requires accurate kinetic models. Many studies [8–28] build on the Miller and Bowman mechanism [29], refining NH_3 models by incorporating new reaction pathways, pressure dependence, and optimized rate parameters. Despite progress, discrepancies persist. Chemical models rely on quantum chemistry and statistical rate theory, validated against experimental data such as ignition delay times (IDT), laminar burning velocities (LBV), and concentrations in jet-stirred reactors (JSR), flow reactors (FR), and burner stabilised flames (BSF). While 0D/1D models suffice for basic simulations, complex combustion devices require Computational Fluid Dynamics (CFD) simulations, which demand compact mechanisms due to computational constraints. Simplifying kinetic models by retaining only essential species and reactions helps reduce simulation costs [30–34].

Pioneers like Frenklach et al [35,36], Sheen and Wang [37,38], Turányi et al. [39], and Pitsch and coworkers [40] advanced kinetic parameter optimization, leading to tools like the ReSpecTh information system and the Optima++ code assisting combustion model development. This work aims to develop a compact NH_3/H_2 reaction mechanism with high predictive accuracy for CFD simulations, optimizing the San Diego kinetic model [35] (21 species, 64 reactions) due to its small size and satisfactory predictive performance across various conditions, based on the findings of Szanthoffer et al. [41].

2. Methods – Kinetic model optimization

Turányi et al. proposed the following experimental uncertainty normalised mean square error function [39], and implemented into code Optima++ [39,42,43] for performance evaluation and parameter optimization of combustion kinetic models:

$$E(\boldsymbol{P}) = \frac{1}{N}\sum_{f=1}^{N_f}\sum_{s=1}^{N_{fs}}\frac{w_{fs}}{N_{fsd}}\sum_{d=1}^{N_{fsd}}\left(\frac{Y_{fsd}^{\mathrm{sim}}(\mathbf{P})-Y_{fsd}^{\mathrm{exp}}}{\sigma(Y_{fsd}^{\mathrm{exp}})}\right)^2 . \quad (1)$$

N, N_f , N_{fs}, N_{fsd} are the number of data series in all RKD data files, the number of files, the number of data series in the fth file, and the number of data in the sth data series of the fth file, respectively. Y_{fsd}^{exp} and $\sigma(Y_{fsd}^{\mathrm{exp}})$ are the dth experimental data in the sth data series of the fth file and its one standard deviation uncertainty, respectively. $Y_{fsd}^{\mathrm{sim}}(\mathbf{P})$ is the corresponding value simulated by the investigated kinetic model at vector of model parameter values $\mathbf{P}$. Non-unit w_{fs} weights can correct biases arising from highly imbalanced data quantities.

The Optima++ code utilises the robust FOCTOPUS global optimization algorithm [44,45] to fit the model predictions to experimental data. The value of the error function has an absolute meaning, as $\sqrt{E}$ measures the uncertainty normalised root-mean-square deviation ("RMSD error") between the model and the experimental results, thus for the "perfect" model $\sqrt{E} \leq 1$, if $\sqrt{E} \approx 2$ the model is usually considered a great model, and a model is considered satisfactorily predictive if $\sqrt{E} < 3$. The error function can also be evaluated also for each type of measurements.

The influential reactions are usually identified by local sensitivity analysis of the simulation results with respect to the rate coefficients (e.g. A_j pre-exponential factors) [46], which ranks reactions based on their log-normalised local sensitivity coefficient:

$$S_{fsd,j} = \frac{\partial \ln Y_{fsd}^{\mathrm{sim}}}{\partial \ln P_j}. \quad (2)$$

There are more advanced methods, such as the PCALIN method [47] which inherently also accounts for the uncertainty of the rate coefficients and experimental data while also incorporating all normalization and weighting within the error function.

Due to the small size of the San Diego 2018 mechanism, it inevitably misses important chemical pathways. Consequently, even if its rate parameters had the physically exact values, its performance would be suboptimal. Therefore, a non-physical, ±1 order of magnitude uncertainty range was defined around the initial rate coefficient curves in the temperature range of 500–2500 K, to allow maximum compensation of the missing mechanistic details. During optimization, this uncertainty range was sampled uniformly in ln$A$, n and E/R transformed Arrhenius parameters as proposed by Nagy et al. [45]. It is important to note that all the kinetic mechanisms poorly describe ammonia's strong collider properties, which results in unusually large (e.g. 5–20 relative to N_2 or Ar) temperature-dependent third-body efficiencies [48–50]. Thus, their good accuracy is often achieved through off-tuned rate coefficients that compensate for these gaps.

Finally, the performance of the improved San Diego 2018 reaction mechanism developed in this study was evaluated by assessing its accuracy against 21 reaction mechanisms from the literature [8–28].

3. Experimental data and its uncertainty

To develop an improved model with robust performance for different burner designs, a large collection of NH_3/H_2 LBV, and concentration data measured in JSRs and burner-stabilised stagnation flames (BSSF) were considered as optimisation targets. All JSR data and a large part of the LBV data have been collected and previously used for model performance evaluation by Szanthoffer et al. [41,77], encoded into RKD format data files [78], and stored in the ReSpecTh database [79]. The newly collected data (LBV and BSSF) has also been encoded into RKD files and are available in the ReSpecTh database with the publication. The total number of RKD files (N_{files}), experiments (N_{exp}), data series (N_{series}), and data points (N_{data}) and the covered ranges of conditions are shown in Table 1.

Regarding BSSF measurements, only a single data series for 70/30 vol% NH_3/H_2 mixtures was used, as measured by Hayakawa et al. [75]. This ratio optimises combustion by combining ammonia's high energy density and carbon-free nature with hydrogen's fast flame speed and wide flammability range. Due to the significant disagreement in the measured concentration values for combustion of pure NH_3 fuel in JSR experiments of different laboratories, only data for NH_3/H_2 mixtures, measured by Zhang et al. [23] and Osipova et al. [76], were considered. LBV measurements available from 26 publications are listed in Table 2 together with the applied method.

A method for the a posteriori assessment of statistical noise in a data series ($\sigma_{fs,\text{stat}}$ for the sth data series in f^{th} RKD file) was carried out using the Minimal Spline Fit code [80]. This value was combined with the reported experimental uncertainty ($\sigma_{fsd,\text{exp}}$) using the formula of Olm et al. [81] to give a more conservative estimate for the uncertainty:

$$\sigma\left(Y_{fsd}^{\text{exp}}\right) = \sqrt{\sigma_{fs,\text{stat}}^2 + \sigma_{fsd,\text{exp}}^2} \ . \tag{3}$$

This procedure was followed by Szanthoffer et al. [41] and also in this work for the previously and newly collected experimental data, respectively.

4. Methods – Accelerated flame simulations

Model optimization involving many active parameters, require numerous repeated simulations using the same mechanism with modified parameters. A comprehensive database of numerical simulation results is established in Optima++ using Cantera 2.6 solver [82] to reduce the computational overhead of

Table 1
Optimisation targets from different reactor types used in the current study (used/total)

Measurement	Publication	Ref.	N_{files}	N_{series}	N_{exp}	N_{data}	x_{H2}%	φ	p/atm	T or T_u/K
BSSF conc.	Hayakawa et al. 2022	[75]	1	7	17	119	30	0.57-1.40	1	298
JSR conc.	Zhang et al. 2021	[23]	8	14	71/74	284/296	10-70	0.15-0.79	1	800-1281
	Osipova et al. 2022	[76]	3	33	51/54	254/269	38-61	0.60-1.50	1	800-1300
LBV	See Table 2.	-	179	179	1283	1283	0-100	0.20-2.00	1.0-36.6	295-584
All	TOTAL	-	191	233	1416	1940	0-100	0.20-2.00	1.0-36.6	295-1281

Table 2
Laminar burning velocity measurement considered in the current study

#	Publication	Ref.	Method[a]	N_{files}	N_{data}	x_{H2}%	φ	p/atm	T_u/K
1	Lee et al. 2009	[51]	OPF	5	10	10-50	0.6-1.67	1.0	298
2	Lee et al. 2010	[52]	OPF	3	15	69-100	0.6-1.67	1.0	298
3	Hayakawa et al. 2015	[53]	OPF	3	13	0	0.8-1.2	1.0-4.9	298
4	Ichikawa et al. 2015	[54]	OPF	3	22	0-100	1.0	1.0-4.9	298
5	Li et al. 2018	[55]	OPF	1	6	0	0.8-1.3	1.0	300
6	Han et al. 2019	[56]	HF	6	99	0-45	0.7-1.6	1.0	298
7	Liu et al. 2019	[57]	OPF	5	26	0	0.2-2.0	0.5-1.6	298
8	Mei et al. 2019	[58]	OPF	7	51	0	0.6-1.5	1.0-5.0	298
9	Han et al. 2020	[59]	HF	7	63	0	0.7-1.5	1.0	298-448
10	Lesmana et al. 2020	[60]	FC	3	21	0-8	0.9-1.2	1.0	295
11	Lhuillier et al. 2020	[61]	OPF	35	240	5-60	0.8-1.4	1.0	298-473
12	S. Wang et al. 2020	[62]	HF	5	67	40-60	0.6-1.6	1.0-4.9	298
13	D. Wang et al. 2020	[63]	OPF	9	51	0	0.6-1.4	1.0	303-393
14	Xia et al. 2020	[64]	OPF	2	15	0	0.6-1.6	1.0	298
15	Kim et al. 2021	[65]	OPF	3	12	0	0.9-1.2	1.0	298
16	Li et al. 2021	[66]	OPF	4	22	0	0.6-1.4	1.0	300
17	Mei et al. 2021	[24]	OPF	7	40	14-86	0.7-1.4	1.0-10.0	298
18	Osipova et al. 2021	[67]	FC	1	9	30	0.7-1.5	1.0	368
19	Shrestha et al. 2021	[68]	OPF	23	105	0-30	0.8-1.4	1.0-9.4	298-476
20	N. Wang et al. 2021	[69]	OPF	3	17	10-20	0.5-1.5	1.0-4.9	360
21	Gotama et al. 2022	[13]	OPF	2	14	40	0.8-1.8	1.0-4.9	298
22	Han et al. 2022	[70]	HF	4	49	4-60	0.6-1.6	1.0	298
23	Hou et al. 2022	[71]	OPF	6	32	0	0.7-1.3	1.0-14.8	298
24	Ji et al. 2022	[72]	OPF	10	92	0-87	0.6-2.0	1.0	303
25	Karan et al. 2022	[73]	OPF	14	140[b]	0	0.8-1.3	2.0-36.6	369-584
26	Zitouni et al. 2023	[74]	OPF	8	52	0-80	0.6-1.4	1.0	298

[a] OPF: Outwardly Propagating spherical Flame method, HF: Heat Flux method, FC: Flame Cone method.
[b] Originally published 2102 data points in 14 series were subsampled, resulting 10 points in each series.

repeated simulations. Given the large number of flame conditions (1283 experiments) and the extensive repeated simulations required for the optimization, it was necessary to further accelerate the simulations. Consequently, as a compromise between accuracy and fast simulations free from convergence issues, loose thresholds for gradient (0.06) and curvature (0.12) convergence criteria were employed and thermal radiation was neglected during optimization, which was shown to cause 5% variation in the RMSD error value for LBV, thus, it is an acceptable trade-off, as significantly larger improvements are realised following parameter optimization (see later). Sensitivity analysis was carried out using tight thresholds (GRAD = 0.01, CURV = 0.02).

5. Methods – CFD simulations

This section describes the numerical setup for the CFD simulation of a turbulent swirl flame, with a constant burning power of 10 kW and selected equivalence ratios of 0.6, 0.8, 1.0, and 1.2. The novel burner geometry and experimental setup were presented in detail by Mashruk et al. [83]. The raw experimental data from [83] were standardised using the averaged oxygen and water content and presented as 15 vol% O_2 on a dry gas basis. The simulations were conducted using Ansys Fluent 2024r1 [84] with the Reynolds-averaged Navier-Stokes (RANS) approach and the Reynolds Stress Model (RSM) for turbulence. The Stress-Menters Baseline (Stress-BSL) model was selected to represent the pressure-strain term in the transport equation for stresses. The reacting flow calculations used the Eddy Dissipation Concept (EDC) combustion model. Calculations were performed using the default turbulent Schmidt number value (0.7) and including thermal diffusion.

The calculations included the determination of heat transfer rates for the burner and quartz glass at a temperature of 288 K, with and a heat transfer coefficient of 20 W/m²K. The radiative heat flux was modelled using the Discrete Ordinates (DO) model. In consideration of the heat and flow models applied, the coupled pressure-velocity solver was employed with the Procedure for Efficient Solution of Transient and Steady-State Operations (PRESTO!) scheme for pressure discretization, and a second-order scheme was used for the remaining equations.

The improved mechanism presented in this work was compared to the Stagni et al. 2020 [28] and Nakamura et al. 2019 [27] mechanisms, which were selected for their relatively small size, overall good performance, and very good predictive capability for emissions in ammonia-hydrogen flames [85,86].

A 40-degree rotationally periodic section of the combustor above was represented with a three-dimensional mesh of 1.6 million polyhedral elements for a radial cross-section (see Fig. 2). Simulations were carried out for a fully premixed mode of the burner operation, which allowed the mesh size to be reduced but neglected possible inhomogeneities in the

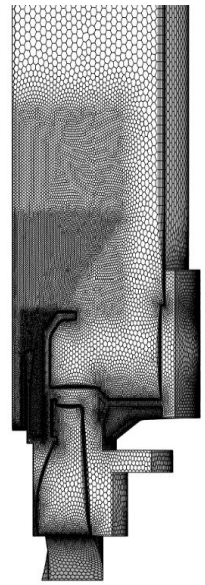

Fig. 2. Radial cross-section of a 40-degree periodic burner section showing the computational grid structure and domain configuration.

H_2 distribution, which in the experimental setup is supplied near the tangential swirler for safety reasons. A significant densification of the grid was performed for the region surrounding the projected flame position, the tangential swirler and the boundary layer near possible separation points.

6. Results – Kinetic model optimization

In addition to the San Diego 2018 mechanism, 20 NH_3/H_2 mechanisms published since 2018 were collected from the literature to evaluate the performance of the optimised model (Present work, PW mechanism). The list of the considered "decarbonised" mechanisms (i.e no carbon atom containing species) are shown in Table 3.

To identify influential reactions whose rate coefficients should be optimised, sensitivity analysis was carried out on the whole data collection using +5% perturbation on the pre-exponential factor of all rate coefficients (64+5 for low-pressure limit). Both standard sensitivity analysis and the PCALIN method showed that each of the 69 rate coefficients had a significant influence on the simulation results, thus, all three Arrhenius parameters of all rate coefficients were considered in the optimization to exploit maximum flexibility of the model to compensate for the mechanistic deficiencies. To account for the imbalance in the data collection, during optimization, the error function weights in Eq. (1) were set to 1/179, 1/47 and 1/7 for the 179 LBV, 47 JSR and 7 BSSF data series, respectively.

Table 3 presents the performance the mechanisms in terms of $\sqrt{E}$ evaluated for the three types of measurements separately, and the overall error

Table 3
Prediction errors of the investigated kinetic models for BSSF and JSR concentration measurements

#	Mechanism	N_{spec}	N_{reac}	$\sqrt{E_{LBV}}$	$\sqrt{E_{JSR}}$	$\sqrt{E_{BSSF}}$	$\sqrt{E_{Overall}}$	$\sqrt{E_{JSR}}$							$\sqrt{E_{BSSF}}$						
								NH_3	H_2	O_2	H_2O	N_2	NO	N_2O	NH_3	H_2	O_2	H_2O	NO	NO_2	N_2O
1	Zhu 2024	39	312	2.97	1.11	2.27	2.25	2.1	0.8	0.8	1.4	0.6	0.4	0.5	0.9	0.9	1.3	1.9	0.7	1.5	5.2
2	Han 2023	32	171	2.24	1.63	3.70	2.67	2.5	0.8	0.6	1.3	0.9	0.7	2.8	1.1	5.4	0.7	3.9	6.3	3.0	1.0
3	Present work	21	64	1.97	2.72	3.24	2.70	4.0	2.3	2.9	3.3	2.7	1.3	1.5	0.7	5.6	0.8	3.9	1.5	3.6	3.2
4	Jian 2024	32	233	3.23	1.80	3.79	3.06	2.2	2.6	1.0	1.3	2.8	0.5	0.5	1.8	5.1	0.7	4.0	2.8	2.2	6.5
5	Otomo 2018	32	213	3.67	2.03	3.65	3.21	2.9	1.4	2.5	2.3	2.4	0.5	1.0	0.8	5.3	0.8	3.8	5.4	1.9	4.1
6	X. Zhang 2021	34	224	2.45	2.78	4.59	3.41	3.5	2.8	1.3	3.1	3.5	1.1	3.0	1.3	5.6	0.7	3.8	3.9	2.8	8.7
7	Stagni 2023	31	203	3.46	1.75	4.69	3.51	2.0	1.3	0.8	1.8	2.1	0.6	2.7	1.5	5.4	0.7	4.0	3.3	2.7	9.4
8	Gotama 2022	32	165	3.28	2.91	4.59	3.67	2.9	3.7	2.1	2.4	1.2	1.2	5.0	1.0	5.6	0.7	3.8	5.1	3.1	8.1
9	Nakamura 2019	34	229	3.75	2.87	4.71	3.85	3.9	3.6	0.9	4.2	3.0	0.6	1.4	2.7	5.3	0.7	4.0	2.7	2.7	9.4
10	Stagni 2020	31	203	3.32	3.31	4.90	3.91	2.0	1.3	0.5	1.6	1.5	0.7	8.1	1.1	5.7	0.7	3.8	7.2	2.8	7.6
11	Liu 2024	35	238	3.96	2.39	5.19	4.01	2.7	1.4	1.4	2.7	1.1	1.2	4.3	1.5	5.5	0.7	3.9	6.2	3.2	9.6
12	Glarborg 2022	34	227	6.42	2.55	4.45	4.74	3.1	2.4	1.2	2.8	3.2	1.4	2.9	2.1	5.3	0.8	4.1	1.8	2.2	9.0
13	Glarborg 2023	34	228	6.52	2.54	4.45	4.79	3.1	2.4	1.2	2.8	3.2	1.4	2.9	2.2	5.3	0.8	4.0	1.8	2.2	9.0
14	He 2023	34	221	7.37	2.46	4.45	5.17	3.2	2.7	1.1	2.7	3.1	1.0	2.4	2.9	4.1	0.8	3.9	2.5	2.3	9.3
15	Z. Zhang 2024	34	224	8.46	1.14	4.50	5.57	2.1	0.6	1.1	1.5	0.6	0.5	0.4	3.1	4.1	0.7	4.0	2.9	2.4	9.2
16	Mei 2021	35	239	4.02	1.65	9.84	6.21	2.3	1.7	2.0	1.6	1.8	0.6	0.8	17.1	6.1	9.4	10.4	1.8	3.6	11.6
17	Wang 2022	32	140	2.53	2.64	10.13	6.22	3.6	3.5	2.7	3.0	2.0	1.5	0.9	17.2	8.2	9.3	10.9	5.1	3.8	10.5
18	Tamaoki 2024	33	228	3.29	2.14	10.17	6.29	2.9	1.2	2.3	1.8	2.3	1.8	2.3	17.2	8.2	9.3	10.8	5.7	3.8	10.5
19	Meng 2023	39	269	10.14	3.11	4.62	6.68	4.1	2.4	1.6	4.1	3.6	1.3	3.4	2.9	5.1	0.8	4.1	2.5	2.4	9.3
20	Klippenstein 2018	33	108	10.28	3.03	4.73	6.76	4.1	2.4	1.6	4.1	3.6	1.3	2.8	2.9	5.1	0.8	4.2	2.9	2.2	9.6
21	Glarborg 2018	33	211	10.29	3.03	4.73	6.77	4.1	2.4	1.6	4.1	3.6	1.3	2.8	2.9	5.1	0.8	4.1	2.9	2.2	9.6
22	San Diego 2018	21	64	3.36	2.43	13.94	8.40	2.8	3.1	1.1	3.1	1.0	0.7	3.4	24.9	10.1	12.3	15.8	9.7	5.5	10.7

Green-yellow-red highlighting of cells corresponds to $\sqrt{E}$=2, 3, 4 error values, respectively.

function value ($\sqrt{E_{\mathrm{Overall}}}$) was calculated as the root mean square average of the three errors. The accuracy of the PW mechanism has been greatly improved compared to the San Diego 2018 mechanism in predicting LBVs. Surprisingly, it has become the most accurate mechanism for LBV calculation despite its smallest size. Very good performance is shown also by Han 2023 and the Z. Wang 2022 mechanisms, but the simulations using these mechanisms take at least five times longer than those using the PW mechanism.

The average performance in predicting JSR concentrations for NH_3/H_2 mixtures with at least 10 vol% H_2 content is acceptable for all models. Notably, the Zhu 2024 and Z. Zhang 2024 mechanisms provided especially accurate descriptions ($\sqrt{E} \sim 1$). Additionally, the Han 2023, Mei 2021, Stagni 2023, Jian 2018, Otomo 2018, and Tamaoki 2024 mechanisms performed well ($\sqrt{E} \sim 1.5$–2.1). The San Diego 2018 mechanism shows fair performance with $\sqrt{E} = 2.43$, with slight deterioration upon optimization ($\sqrt{E} = 2.72$), yet its error remains below 3.

In predicting BSSF concentration data, except for the most detailed Zhu 2024 mechanism ($\sqrt{E} = 2.27$), all mechanisms had unsatisfactory performance ($\sqrt{E} \geq 3.65$). While the San Diego 2018 mechanism had the highest error value of $\sqrt{E} = 13.9$, the PW mechanism emerged as the second-best one among the 22 mechanisms with $\sqrt{E} = 3.24$ for BSSF. Table shows the prediction errors of the mechanisms for the concentrations of different species measured in JSR and BSSF experiments. Regarding JSR experiments, the PW mechanism has very accurate predictions for NO and N_2O ($\sqrt{E} \leq 1.5$), and acceptable predictions for H_2, O_2, H_2O and N_2. Its accuracy for NH_3 deteriorated significantly compared to the San Diego 2018 model ($\sqrt{E} = 2.8 \rightarrow 4.0$), however, surprisingly, none of the mechanisms can perform excellently in this regard (all $\sqrt{E} \geq 2$). Good descriptions are given only by the Stagni 2020, Stagni 2023, Zhu 2024, Z. Zhang 2024 and Jian 2024 mechanisms.

Regarding NO emissions, all mechanisms perform well or excellently. For N_2O, only eight mechanisms, including the PW mechanism, can give accurate estimates ($\sqrt{E} < 2$), and five models, including the San Diego 2018 mechanism were unreliable ($\sqrt{E} \geq 3.4$. For O_2 concentrations, almost all mechanisms perform accurately, and four mechanisms, including the PW model, have acceptable performance. For H_2 concentrations, the predictions are also generally good or at least acceptable, and only the Gotama 2022, Nakamura 2019, Wang 2022, and San Diego 2018 mechanisms have unacceptably large errors ($\sqrt{E} > 3$). In summary, three mechanisms: the Zhu 2024, the Z. Zhang 2024, and the Mei 2021 mechanisms showed reliable performance for all seven species.

Regarding BSSF concentration measurements, the Zhu 2024 mechanism clearly stands out with its universal high accuracy for all species apart from N_2O. For H_2 and H_2O, all other mechanisms give bad predictions ($\sqrt{E} \geq 4.1$ and 3.8). For N_2O, only the Han 2023 ($\sqrt{E} = 1$) and PW ($\sqrt{E} = 3.2$) mechanisms show good and acceptable performances, respectively, whereas all other mechanisms perform poorly ($\sqrt{E} \geq 4.1$). Except for four mechanisms (Mei 2021, Wang 2022, Tamaoki 2024, San Diego 2018), all models give good or acceptable predictions for NH_3, with the PW emerging as the best. The trend is similar for O_2: all mechanisms, except for the same four models, give excellent predictions. These four bad performing mechanisms and the PW model are also inaccurate ($\sqrt{E} \geq 3.6$) for NO_2, whereas most models predict it relatively accurately or at least acceptably with an error of $\sqrt{E} = 1.9$–3.2. After Zhu 2024, the PW model has the best performance for NO ($\sqrt{E} = 1.5$), whereas half of the mechanisms perform badly ($\sqrt{E} \geq 3.0$).

7. Results – CFD simulations

The CFD simulations of 70/30 vol% NH_3/H_2 mixture were carried out for a swirl burner at 0.6, 0.8,

1.0. and 1.2 equivalence ratios. In the simulations, the tested mechanisms provided similar flow fields and temperature distributions across all the tested equivalence ratios. Figure 3 summarises the simulation result for outlet concentrations of NH_3 and the three main NO_x species obtained by the three mechanisms in comparison with the experimentally measured values. Emissions are normalised to a reference oxygen concentration of 15 vol% in the dry exhaust, which excludes water vapor.

Regarding NO emissions in the ϕ = 0.8–1.2 range, all mechanisms perform qualitatively well, with the Stagni 2020 mechanism demonstrating the best accuracy, whereas the other two significantly overpredict peak NO emissions in almost perfect agreement with each other. While all mechanisms demonstrated the highest NO emission at 0.8, the NO emission drop observed at very lean conditions was only captured by the improved mechanism. At very lean conditions, the PW mechanism predicts NH_3 slip accurately, whereas the other two mechanisms predict no slip at all. All mechanisms accurately describe the complete consumption of NH_3 under stoichiometric and slightly lean conditions, and they give a good qualitative description for the unburnt ammonia in rich flames. In the latter case, considering that experimental NH_3 emissions exceed the measurement limits, the present mechanism and the Stagni 2020 mechanism provide the best and second best predictions, while the Nakamura 2019 model underpredicts the result by at least one order of magnitude. Regarding N_2O concentration predictions, all mechanisms are qualitatively correct as they give zero emissions only in the ϕ = 0.8–1.2 range. The Nakamura 2019 mechanism is the most accurate, with 20% overprediction, whereas the PW mechanism and the Stagni 2020 mechanism overpredict by 80% and 170%, respectively, compared to the experiment. Regarding NO_2 concentration all models reproduce zero emissions at stoichiometric and rich conditions. All mechanisms predict the emergence of emission at ϕ=0.8, however, they yield 3-4 times lower values than the experimental data. The Nakamura 2019 and the Stagni 2020 mechanisms give monotonically increasing emission with decreasing equivalence ratio, while the PW mechanism accurately captures the decreasing trend under very lean conditions.

In summary, the PW model captures the NH_3 slip and the rapid NO decrease at an equivalence ratio of 0.6, and it also shows good qualitative agreement with the N_2O and NO_2 concentrations. It should be noted that the resulting NO_2 emissions were under-predicted, falling within the range of a few ppm, so this trend requires further investigation for confirmation. However, given the limited number of data points, especially in regions with large gradients, such as very lean and near stoichiometric conditions, these predictions should be viewed as an indication of the mechanism's capabilities rather than a direct fit.

The PW mechanism is highly efficient, running 1.78–2.14 times faster than the Nakamura 2019 and Stagni 2020 models while maintaining accurate pollutant emission predictions.

8. Conclusions

In this study, it was found that the mediocre accuracy of the compact San Diego 2018 mechanism

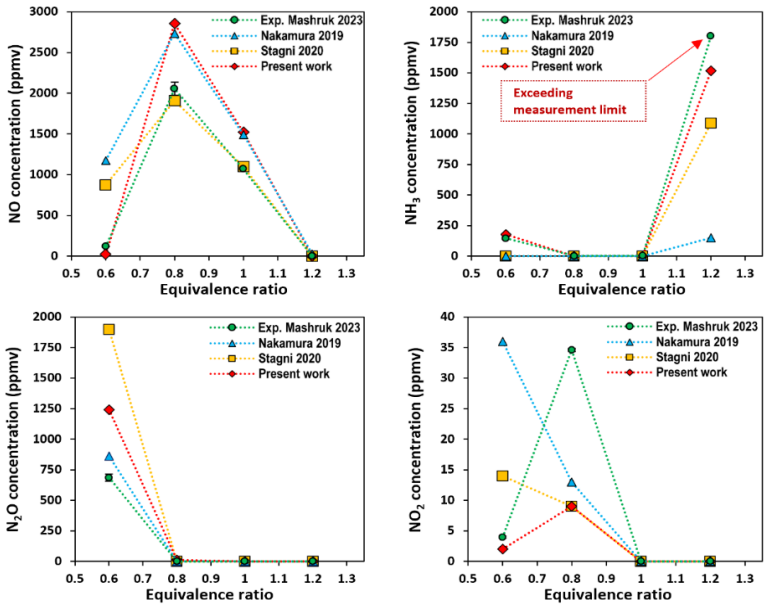

Fig. 3. Outlet concentration of NH_3, NO, N_2O, and NO_2 species measured experimentally by Mashruk et al. [83] and calculated using CFD simulations with three mechanisms (PW: present work) for 70/30 vol% NH_3/H_2 blends in a swirl burner design. Emissions are

in predicting LBVs, and concentrations in JSRs and BSSFs could be greatly improved by rate parameter optimization if unphysically wide tuning ranges are allowed for its rate coefficients. The optimised model showed the best performance for LBV and gave reliable predictions for NH_3, NO and N_2O in BSSF and for NO and N_2O in JSR, but its performance for NO_2 in BSSF and for NH_3 in JSR still needs to be improved. The model has also been tested in computational fluid dynamics simulations of a swirl burner, and it allowed rapid simulations there as well. Its predictions showed excellent qualitative and often good quantitative agreement with the experimentally measured emissions, which could not be provided by other widely used mechanisms.

Despite the improved performance of the optimized San Diego 2018 model, tuning alone cannot fully compensate for missing reaction pathways. Future improvements include expanding its chemistry and parameterization, particularly with pressure-dependent descriptions and third-body efficiencies for key reactions like NH_3. Given its structural deficiencies, the optimized rate parameters are not physically recommended, but the mechanism offers a good balance between accuracy and efficiency for CFD applications.

Acknowledgments

The authors express their gratitude for the support received from EPSRC through the SAFE-AGT Pilot project (No. EP/T009314/1) and the Green Ammonia Thermal Propulsion MariNH3 project (No. EP/W016656/1), Ali Alnasif also extends his thanks to Al-Furat Al-Awsat Technical University (ATU) for financially supporting his PhD studies in the UK. T. Nagy and T. Turányi thank the support of the National Research, Development, and Innovation Fund (NKFIH) FK134332 and K147024 grants, respectively. A. Gy. Szanthoffer was supported by the DKOP-23 Doctoral Excellence Program of the Ministry for Culture and Innovation of Hungary from NKFIH. Joanna Jójka acknowledges funding for her doctoral fellowship from the National Science Center, Poland (UMO-2019/32/T/ST8/00265).

References

[1] A. Valera-Medina, F. Amer-Hatem, A.K. Azad, I.C. Dedoussi, M. De Joannon, R.X. Fernandes, P. Glarborg, H. Hashemi, X. He, S. Mashruk, J. McGowan, C. Mounaim-Rouselle, A. Ortiz-Prado, A. Ortiz-Valera, I. Rossetti, B. Shu, M. Yehia, H. Xiao, M. Costa, Review on ammonia as a potential fuel: From synthesis to economics, Energy and Fuels 35 (2021) 6964–7029.

[2] A. Valera-Medina, H. Xiao, M. Owen-Jones, W.I.F. David, P.J. Bowen, Ammonia for power, Prog Energy Combust Sci 69 (2018) 63–102.

[3] W.S. Chai, Y. Bao, P. Jin, G. Tang, L. Zhou, A review on ammonia, ammonia-hydrogen and ammonia-methane fuels, Renewable and Sustainable Energy Reviews 147 (2021).

[4] H. Kobayashi, A. Hayakawa, K.D.K.A. Somarathne, E.C. Okafor, Science and technology of ammonia combustion, Proceedings of the Combustion Institute 37 (2019) 109–133.

[5] J. Li, S. Lai, D. Chen, R. Wu, N. Kobayashi, L. Deng, H. Huang, A Review on Combustion Characteristics of Ammonia as a Carbon-Free Fuel, (n.d.).

[6] L. Cox, Nitrogen oxides (NOx) why and how they are controlled, Diane Publishing, 1999.

[7] J. Fritt-Rasmussen, K. Gustavson, P.J. Aastrup, M.D. Agersted, D. Boertmann, D.S. Clausen, C.J. Jørgensen, A.S. Lansø, A. Mosbech, Assessment of the potential environmental impacts of a major ammonia spill from a Power-to-X plant and from shipping of ammonia in Greenland, Aarhus University, DCE - Danish Centre for Environment and Energy, 2022.

[8] Y. Zhu, H.J. Curran, S. Girhe, Y. Murakami, H. Pitsch, K. Senecal, L. Yang, C.W. Zhou, The combustion chemistry of ammonia and ammonia/hydrogen mixtures: A comprehensive chemical kinetic modeling study, Combust Flame 260 (2024).

[9] X. Han, Z. Wang, B. Zhou, Y. He, Y. Zhu, K. Cen, Effect of H2 and O2 enrichment on the laminar burning velocities of NH3+H2+N2+O2 flames: Experimental and kinetic study, Applications in Energy and Combustion Science 15 (2023).

[10] J. Jian, H. Hashemi, H. Wu, P. Glarborg, A.W. Jasper, S.J. Klippenstein, An experimental, theoretical, and kinetic modeling study of post-flame oxidation of ammonia, Combust Flame 261 (2024).

[11] J. Otomo, M. Koshi, T. Mitsumori, H. Iwasaki, K. Yamada, Chemical kinetic modeling of ammonia oxidation with improved reaction mechanism for ammonia/air and ammonia/hydrogen/air combustion, Int J Hydrogen Energy 43 (2018) 3004–3014.

[12] A. Stagni, S. Arunthanayothin, M. Dehue, O. Herbinet, F. Battin-Leclerc, P. Bréquigny, C. Mounaïm-Rousselle, T. Faravelli, Low- and intermediate-temperature ammonia/hydrogen oxidation in a flow reactor: Experiments and a wide-range kinetic modeling, Chemical Engineering Journal 471 (2023).

[13] G.J. Gotama, A. Hayakawa, E.C. Okafor, R. Kanoshima, M. Hayashi, T. Kudo, H. Kobayashi, Measurement of the laminar burning velocity and kinetics study of the importance of the hydrogen recovery mechanism of ammonia/hydrogen/air premixed flames, Combust Flame 236 (2022).

[14] B. Liu, Z. Zhang, S. Yang, F. Yu, B.Y. Belal, G. Li, Experimental and chemical kinetic study for the combustion of ammonia-hydrogen mixtures, Fuel 371 (2024) 131850.

[15] P. Glarborg, The NH3/NO2/O2 system: Constraining key steps in ammonia ignition and N2O formation, Combust Flame 257 (2023).

[16] X. He, M. Li, B. Shu, R. Fernandes, K. Moshammer, Exploring the Effect of Different Reactivity Promoters on the Oxidation of Ammonia in a Jet-Stirred Reactor, Journal of Physical Chemistry A 127 (2023) 1923–1940.

[17] Z. Zhang, A. Li, Z. Li, F. Ren, L. Zhu, Z. Huang, An experimental and kinetic modelling study on the oxidation of NH3, NH3/H2, NH3/CH4 in a variable pressure laminar flow reactor at engine-relevant conditions, Combust Flame 265 (2024) 113513.

[18] S. Wang, Z. Wang, C. Chen, A.M. Elbaz, Z. Sun, W.L. Roberts, Applying heat flux method to laminar burning velocity measurements of NH3/CH4/air at elevated pressures and kinetic modeling study, Combust Flame 236 (2022).

[19] Q. Meng, L. Lei, J. Lee, M.P. Burke, On the role of HNNO in NOx formation, Proceedings of the Combustion Institute 39 (2023) 551–560.

[20] S.J. Klippenstein, M. Pfeifle, A.W. Jasper, P. Glarborg, Theory and modeling of relevance to prompt-NO formation at high pressure, Combust Flame 195 (2018) 3–17.

[21] P. Glarborg, J.A. Miller, B. Ruscic, S.J. Klippenstein, Modeling nitrogen chemistry in combustion, Prog Energy Combust Sci 67 (2018) 31–68.

[22] Mechanical and Aerospace Engineering (Combustion Research), University of California at San Diego, Chemical-Kinetic Mechanisms for Combustion Applications, Https://Web.Eng.Ucsd.Edu/Mae/Groups/Combustion/Mechanism.Html (2018).

[23] X. Zhang, S.P. Moosakutty, R.P. Rajan, M. Younes, S.M. Sarathy, Combustion chemistry of ammonia/hydrogen mixtures: Jet-stirred reactor measurements and comprehensive kinetic modeling, Combust Flame 234 (2021) 111653.

[24] B. Mei, J. Zhang, X. Shi, Z. Xi, Y. Li, Enhancement of ammonia combustion with partial fuel cracking strategy: Laminar flame propagation and kinetic modeling investigation of NH3/H2/N2/air mixtures up to 10 atm, Combust Flame 231 (2021) 111472.

[25] P. Marshall, P. Glarborg, Probing High-Temperature Amine Chemistry: Is the Reaction NH3+ NH2⇄ N2H3+ H2Important?, Journal of Physical Chemistry A 127 (2023).

[26] K. Tamaoki, Y. Murakami, K. Kanayama, T. Tezuka, M. Izumi, H. Nakamura, Roles of NH2 reactions in ammonia oxidation at intermediate temperatures: Experiments and chemical kinetic modeling, Combust Flame 259 (2024) 113177.

[27] H. Nakamura, M. Shindo, Effects of radiation heat loss on laminar premixed ammonia/air flames, Proceedings of the Combustion Institute 37 (2019) 1741–1748.

[28] A. Stagni, C. Cavallotti, S. Arunthanayothin, Y. Song, O. Herbinet, F. Battin-Leclerc, T. Faravelli, An experimental, theoretical and kinetic-modeling study of the gas-phase oxidation of ammonia, React Chem Eng 5 (2020).

[29] J.A. Miller, C.T. Bowman, Mechanism and modeling of nitrogen chemistry in combustion, Prog Energy Combust Sci 15 (1989) 287–338.

[30] C. Duynslaegher, F. Contino, J. Vandooren, H. Jeanmart, Modeling of ammonia combustion at low pressure, Combust Flame 159 (2012) 2799–2805.

[31] R.C. da Rocha, M. Costa, X.S. Bai, Chemical kinetic modelling of ammonia/hydrogen/air ignition, premixed flame propagation and NO emission, Fuel 246 (2019) 24–33.

[32] H. Xiao, A. Valera-Medina, P. Bowen, S. Dooley, 3D simulation of ammonia combustion in a lean premixed swirl burner, Energy Procedia 142 (2017) 1294–1299.

[33] T. Nagy, T. Turányi, Reduction of very large reaction mechanisms using methods based on simulation error minimization, Combust Flame 156 (2009) 417–428.

[34] I.Gy. Zsély, T. Nagy, J.M. Simmie, H.J. Curran, Reduction of a detailed kinetic model for the ignition of methane/propane mixtures at gas turbine conditions using simulation error minimization methods, Combust Flame 158 (2011) 1469–1479.

[35] M. Frenklach, Transforming data into knowledge—process informatics for combustion chemistry, Proceedings of the Combustion Institute 31 (2007) 125–140.

[36] D. Miller, M. Frenklach, Sensitivity analysis and parameter estimation in dynamic modeling of chemical kinetics, Int J Chem Kinet 15 (1983) 677–696.

[37] H. Wang, D.A. Sheen, Combustion kinetic model uncertainty quantification, propagation and minimization, Prog Energy Combust Sci 47 (2015) 1–31.

[38] D.A. Sheen, H. Wang, The method of uncertainty quantification and minimization using polynomial chaos expansions, Combust Flame 158 (2011) 2358–2374.
[39] T. Turányi, T. Nagy, I.Gy. Zsély, M. Cserháti, T. Varga, B.T. Szabó, I. Sedyó, P.T. Kiss, A. Zempléni, H.J. Curran, Determination of rate parameters based on both direct and indirect measurements, Int J Chem Kinet 44 (2012) 284–302.
[40] L. Cai, H. Pitsch, Mechanism optimization based on reaction rate rules, Combust Flame 161 (2014) 405–415.
[41] A.G. Szanthoffer, I.G. Zsély, L. Kawka, M. Papp, T. Turányi, Testing of NH_3/H_2 and NH_3/syngas combustion mechanisms using a large amount of experimental data, Applications in Energy and Combustion Science (2023) 100127.
[42] M. Papp, T. Varga, Á. Busai, I.G. Zsély, T. Nagy, T. Turányi, Optima++ package v2.5: A general C++ framework for performing combustion simulations and mechanism optimization, (2024).
[43] S.K. Goitom, M. Papp, M. Kovács, T. Nagy, I.G. Zsély, T. Turányi, L. Pál, Efficient numerical methods for the optimisation of large kinetic reaction mechanisms, Https://Doi.Org/10.1080/13647830.2022.2110945 26 (2022) 1071–1097.
[44] T. Nagy, T. Turányi, Uncertainty of Arrhenius parameters, Int J Chem Kinet 43 (2011) 359–378.
[45] T. Nagy, É. Valkó, I. Sedyó, I.G. Zsély, M.J. Pilling, T. Turányi, Uncertainty of the rate parameters of several important elementary reactions of the H_2 and syngas combustion systems, Combust Flame 162 (2015) 2059–2076.
[46] A. Saltelli, S. Tarantola, F. Campolongo, M. Ratto, Sensitivity Analysis in Practice. A Guide to Assessing Scientific Models. In: Probability and Statistics Series., Wiley, 2004.
[47] M. Kovács, M. Papp, T. Turányi, T. Nagy, A novel active parameter selection strategy for the efficient optimization of combustion mechanisms, Proceedings of the Combustion Institute 39 (2023) 5259–5267.
[48] A.W. Jasper, Predicting third-body collision efficiencies for water and other polyatomic baths, Faraday Discuss 238 (2022) 68–86.
[49] P. Glarborg, H. Hashemi, S. Cheskis, A.W. Jasper, On the rate constant for NH2+HO2and third-body collision efficiencies for NH2+H(+M) and NH2+NH2(+M), Journal of Physical Chemistry A 125 (2021) 1505–1516.
[50] P. Sabia, M.V. Manna, R. Ragucci, M. de Joannon, Mutual inhibition effect of hydrogen and ammonia in oxidation processes and the role of ammonia as "strong" collider in third-molecular reactions, Int J Hydrogen Energy 45 (2020) 32113–32127.
[51] A. Hayakawa, M. Hayashi, M. Kovaleva, G.J. Gotama, E.C. Okafor, S. Colson, S. Mashruk, A. Valera-Medina, T. Kudo, H. Kobayashi, Experimental and numerical study of product gas and N2O emission characteristics of ammonia/hydrogen/air premixed laminar flames stabilized in a stagnation flow, Proceedings of the Combustion Institute 39 (2023) 1625–1633.
[52] A.G. Szanthoffer, M. Papp, T. Turányi, Identification of well-parameterised reaction steps in detailed combustion mechanisms – A case study of ammonia/air flames, Fuel 380 (2025) 132938.
[53] M. Papp, T. Varga, C. Olm, Á. Busai, T. Nagy, I.Gy. Zsély, T. Turányi, ReSpecTh Kinetics Data Format Specification v2.5, (2024).
[54] ReSpecTh information site, (2024).
[55] K.N. Osipova, X. Zhang, S.M. Sarathy, O.P. Korobeinichev, A.G. Shmakov, Ammonia and ammonia/hydrogen blends oxidation in a jet-stirred reactor: Experimental and numerical study, Fuel 310 (2022) 122202.
[56] A. Karan, G. Dayma, C. Chauveau, F. Halter, Experimental study and numerical validation of oxy-ammonia combustion at elevated temperatures and pressures, Combust Flame 236 (2022).
[57] T. Nagy, T. Turányi, Minimal Spline Fit: a model-free method for determining statistical noise of experimental data series, in: Proceedings of the European Combustion Meeting, Paper 336, 2021.
[58] C. Olm, T. Varga, É. Valkó, H.J. Curran, T. Turányi, Uncertainty quantification of a newly optimized methanol and formaldehyde combustion mechanism, Combust Flame 186 (2017) 45–64.
[59] J.H. Lee, J.H. Kim, J.H. Park, O.C. Kwon, Studies on properties of laminar premixed hydrogen-added ammonia/air flames for hydrogen production, Int J Hydrogen Energy 35 (2010) 1054–1064.
[60] J.H. Lee, S.I. Lee, O.C. Kwon, Effects of ammonia substitution on hydrogen/air flame propagation and emissions, Int J Hydrogen Energy 35 (2010) 11332–11341.
[61] A. Hayakawa, T. Goto, R. Mimoto, Y. Arakawa, T. Kudo, H. Kobayashi, Laminar burning velocity and Markstein length of ammonia/air premixed flames at various pressures, Fuel 159 (2015) 98–106.
[62] A. Ichikawa, A. Hayakawa, Y. Kitagawa, K.D. Kunkuma Amila Somarathne, T. Kudo, H. Kobayashi, Laminar burning velocity and Markstein length of ammonia/hydrogen/air premixed flames at elevated pressures, Int J Hydrogen Energy 40 (2015) 9570–9578.
[63] Y. Li, M. Bi, B. Li, W. Gao, Explosion behaviors of ammonia–air mixtures, Combustion Science and Technology 190 (2018) 1804–1816.
[64] X. Han, Z. Wang, M. Costa, Z. Sun, Y. He, K. Cen, Experimental and kinetic modeling study of laminar burning velocities of NH3/air, NH3/H2/air, NH3/CO/air and NH3/CH4/air premixed flames, Combust Flame 206 (2019) 214–226.
[65] Q. Liu, X. Chen, J. Huang, Y. Shen, Y. Zhang, Z. Liu, The characteristics of flame propagation in ammonia/oxygen mixtures, J Hazard Mater 363 (2019) 187–196.
[66] B. Mei, X. Zhang, S. Ma, M. Cui, H. Guo, Z. Cao, Y. Li, Experimental and kinetic modeling investigation on the laminar flame propagation of ammonia under oxygen enrichment and elevated pressure conditions, Combust Flame 210 (2019) 236–246.
[67] X. Han, Z. Wang, Y. He, Y. Liu, Y. Zhu, A.A. Konnov, The temperature dependence of the laminar burning velocity and superadiabatic flame temperature phenomenon for NH3/air flames, Combust Flame 217 (2020) 314–320.
[68] H. Lesmana, M. Zhu, Z. Zhang, J. Gao, J. Wu, D. Zhang, Experimental and kinetic modelling studies of laminar flame speed in mixtures of partially dissociated NH3 in air, Fuel 278 (2020) 118428.
[69] C. Lhuillier, P. Brequigny, N. Lamoureux, F. Contino, C. Mounaïm-Rousselle, Experimental investigation on laminar burning velocities of ammonia/hydrogen/air mixtures at elevated temperatures, Fuel 263 (2020).
[70] S. Wang, Z. Wang, A.M. Elbaz, X. Han, Y. He, M. Costa, A.A. Konnov, W.L. Roberts, Experimental study and kinetic analysis of the laminar burning velocity of NH3/syngas/air, NH3/CO/air and NH3/H2/air premixed flames at elevated pressures, Combust Flame 221 (2020) 270–287.
[71] D. Wang, C. Ji, Z. Wang, S. Wang, T. Zhang, J. Yang, Measurement of oxy-ammonia laminar burning velocity at normal and elevated temperatures, Fuel 279 (2020) 118425.
[72] Y. Xia, G. Hashimoto, K. Hadi, N. Hashimoto, A. Hayakawa, H. Kobayashi, O. Fujita, Turbulent burning velocity of ammonia/oxygen/nitrogen premixed flame in O2-enriched air condition, Fuel 268 (2020) 117383.
[73] H.K. Kim, J.W. Ku, Y.J. Ahn, Y.H. Kim, O.C. Kwon, Effects of O2 enrichment on NH3/air flame propagation and emissions, Int J Hydrogen Energy 46 (2021) 23916–23926.
[74] Y. Li, M. Bi, K. Zhang, W. Gao, Effects of nitrogen and argon on ammonia-oxygen explosion, Int J Hydrogen Energy 46 (2021) 21249–21259.
[75] K.N. Osipova, O.P. Korobeinichev, A.G. Shmakov, Chemical structure and laminar burning velocity of atmospheric pressure premixed ammonia/hydrogen flames, Int J Hydrogen Energy 46 (2021) 39942–39954.
[76] K.P. Shrestha, C. Lhuillier, A.A. Barbosa, P. Brequigny, F. Contino, C. Mounaïm-Rousselle, L. Seidel, F. Mauss, An experimental and modeling study of ammonia with enriched oxygen content and ammonia/hydrogen laminar flame speed at elevated pressure and temperature, Proceedings of the Combustion Institute 38 (2021) 2163–2174.
[77] N. Wang, S. Huang, Z. Zhang, T. Li, P. Yi, D. Wu, G. Chen, Laminar burning characteristics of ammonia/hydrogen/air mixtures with laser ignition, Int J Hydrogen Energy 46 (2021) 31879–31893.
[78] X. Han, Z. Wang, Y. He, Y. Zhu, R. Lin, A.A. Konnov, Uniqueness and similarity in flame propagation of pre-dissociated NH3 + air and NH3 + H2 + air mixtures: An experimental and modelling study, Fuel 327 (2022) 125159.
[79] D. Hou, Z. Zhang, Q. Cheng, B. Liu, M. Zhou, G. Li, Experimental and kinetic studies of laminar burning velocities of ammonia with high Lewis number at elevated pressures, Fuel 320 (2022) 123913.
[80] C. Ji, Z. Wang, D. Wang, R. Hou, T. Zhang, S. Wang, Experimental and numerical study on premixed partially dissociated ammonia mixtures. Part I: Laminar burning velocity of NH3/H2/N2/air mixtures, Int J Hydrogen Energy 47 (2022) 4171–4184.
[81] S. Zitouni, P. Brequigny, C. Mounaïm-Rousselle, Influence of hydrogen and methane addition in laminar ammonia premixed flame on burning velocity, Lewis number and Markstein length, Combust Flame 253 (2023) 112786.
[82] D.G. Goodwin, H.K. Moffat, I. Schoegl, R.L. Speth, B.W. Weber, Cantera: An Object-oriented Software Toolkit for Chemical Kinetics, Thermodynamics, and Transport Processes, (2022).
[83] S. Mashruk, A. Alnasif, C. Yu, J. Thatcher, J. Rudman, L. Peronski, C. Meng-Choung, A. Valera-Medina, Combustion Characteristics of a Novel Ammonia Combustor equipped with Stratified Injection for Low Emissions, Journal of Ammonia Energy 1 (2023).
[84] ANSYS Inc., Ansys Fluent Theory Guide, Canonsburg, 2024.
[85] A. Alnasif, S. Mashruk, H. Shi, M. Alnajideen, P. Wang, D. Pugh, A. Valera Medina, Evolution of ammonia reaction mechanisms and modeling parameters: A review, Applications in Energy and Combustion Science 15 (2023) 100175.
[86] A. Alnasif, J. Jójka, S. Mashruk, T. Nagy, A. Valera-Medina, Analysis of the performance of kinetic reaction mechanisms in estimating N2O mole fractions in 70/30 vol% NH3/H2 premixed flames, Fuel 371 (2024) 131897.
[87] A. Alnasif, S. Mashruk, M. Hayashi, J. Jójka, H. Shi, A. Hayakawa, A. Valera-Medina, Performance Investigation of Currently Available Reaction Mechanisms in the Estimation of NO Measurements: A Comparative Study, Energies 2023, Vol. 16, Page 3847 16 (2023) 3847.